Biophysical Journal, Volume *111*

Supplemental Information

Influence of Ganglioside GM1 Concentration on Lipid Clustering and Membrane Properties and Curvature

Dhilon S. Patel, Soohyung Park, Emilia L. Wu, Min Sun Yeom, Göran Widmalm, Jeffery B. Klauda, and Wonpil Im

TABLES

Table S1. Details of sizes and compositions of all systems.

System	% GM1	Temp	System Info.				
			# GM1	# POPC	# Replicas	# Atoms	Initial Box size (Å^3)
$GM1^{10\%}$	10	293	20	180	5	~66,000	80×80×95
$GM1^{20\%}$	20	293	40	160	5	~66,000	80×80×95
$GM1^{30\%}$	30	293	60	140	5	~65,000	82×82×90
$GM1^{10\%B}$	10	293	80	720	1	260,960	156×156×102
$GM1^{20\%B}$	20	293	160	640	1	260,640	151×151×108
$GM1^{30\%B}$	30	293	240	560	1	258,376	147×147×112
$GM1^{10\%B\text{-}330K}$	10	330	80	720	1	260,960	156×156×102
$GM1^{20\%B\text{-}330K}$	20	330	160	640	1	260,640	150×150×110
$GM1^{30\%B\text{-}330K}$	30	330	240	560	1	258,376	147×147×112

Table S2: RMSD (Å) comparison of representative conformations of top three clusters obtained from systems $GM1^{10\%}$, $GM1^{20\%}$, and $GM1^{30\%}$. All GM1 represents comparison of RMSD of top three clusters from all three concentrations.

System	MD clusters	Clust-1	Clust-2	Clust-3
$GM1^{10\%}$	**Clust-1**	0	0.850	0.853
	Clust-2			1.182
$GM1^{20\%}$	**Clust-1**	0	0.862	0.956
	Clust-2			1.33
$GM1^{30\%}$	**Clust-1**	0	0.910	0.868
	Clust-2			1.217
All GM1	**Clust-1**	0	0.910	0.908
	Clust-2			1.202

Table S3: RMSD (Å) comparison of representative conformations of top three clusters obtained from systems $GM1^{10\%}$, $GM1^{20\%}$, and $GM1^{30\%}$ with crystal structures of GM1 in PDB. All GM1 represents comparison of RMSD of top three clusters from all three concentrations with crystal structures of GM1 in PDB.

System	MD Clusters	Crystal structures						
		3chb	**3bwr**	**3ayc**	**2xrq**	**4l6t**	**3m3q**	**1ct1**
$GM1^{10\%}$	**Clust-1**	0.909	1.300	0.932	0.947	0.903	0.978	1.267
	Clust-2	1.327	1.623	1.109	1.318	1.251	1.311	1.477
	Clust-3	1.226	1.067	1.265	1.187	1.216	1.269	1.200
$GM1^{20\%}$	**Clust-1**	0.934	1.324	0.938	0.971	0.924	1.029	1.227
	Clust-2	1.390	1.665	1.142	1.376	1.305	1.355	1.516
	Clust-3	1.244	0.988	1.277	1.200	1.236	1.261	1.239
$GM1^{30\%}$	**Clust-1**	0.865	1.269	0.923	0.921	0.877	0.950	1.240
	Clust-2	1.327	1.623	1.125	1.320	1.257	1.318	1.457
	Clust-3	1.189	1.060	1.211	1.147	1.179	1.243	1.176
All GM1	**Clust-1**	0.865	1.269	0.923	0.921	0.877	0.950	1.240
	Clust-2	1.327	1.623	1.125	1.320	1.257	1.318	1.457
	Clust-3	1.191	0.974	1.264	1.147	1.184	1.240	1.178

Table S4: Effective proton-proton distances (Å) calculated for systems $GM1^{10\%}$, $GM1^{20\%}$, and $GM1^{30\%}$ from MD simulations. For comparison purpose NMR experimental intra- and inter-residue NOE distances for GM1-modified micelles and GM1 in DMSO are given (See Ref. 64 and 65). Average proton-proton distances obtained from seven crystal structures of GM1 oligosaccharides are also given.

Proton-proton distances		**NMR experiment**		**MD systems**			**Crystal Avg.**
		GM1-acetyl micelles	**GM1 in DMSO**	$GM1^{10\%}$	$GM1^{20\%}$	$GM1^{30\%}$	
Gal2-H1	GalNAc-H2	3.0 ± 0.3	3.5 ± 0.4	4.18 ± 0.23	4.18 ± 0.23	4.18 ± 0.23	4.23 ± 0.16
Gal2-H1	GalNAc-H3		2.5 ± 0.3	2.26 ± 0.18	2.26 ± 0.18	2.26 ± 0.18	2.19 ± 0.15
Gal2-H1	GalNAc-HN	3.0 ± 0.3	3.5 ± 0.4	3.11 ± 0.66	3.08 ± 0.65	3.09 ± 0.65	3.38 ± 0.52
Neu5Ac-HO8	Neu5Ac-H6	2.2 ± 0.2	2.4 ± 0.2	2.61 ± 0.79	2.59 ± 0.78	2.58 ± 0.77	2.04 ± 0.08
Neu5Ac-H8	GalNAc-H1		3.1 ± 0.3	5.55 ± 1.24	5.12 ± 1.41	4.93 ± 1.51	2.38 ± 0.29
Neu5Ac-HO8	GalNAc-H1	2.9 ± 0.3	2.6 ± 0.3	3.78 ± 1.96	3.54 ± 2.07	3.39 ± 2.13	2.69 ± 0.22
Neu5Ac-H32	Gal1-H3	2.4 ± 0.2		2.94 ± 0.70	2.77 ± 0.82	2.64 ± 0.90	2.01 ± 0.09
Neu5Ac-H32	Gal1-HO2	3.4 ± 0.3	3.2 ± 0.3	2.97 ± 0.56	2.96 ± 0.58	2.92 ± 0.55	3.19 ± 0.30
GalNAc-HN	GalNAc-H2	2.5 ± 0.3	2.6 ± 0.3	2.58 ± 0.33	2.61 ± 0.31	2.61 ± 0.32	2.97 ± 0.01
GalNAc-HN	Gal1-H2	3.4 ± 0.3	3.6 ± 0.4	3.29 ± 0.56	3.30 ± 0.56	3.29 ± 0.55	3.91 ± 0.54
GalNAc-H1	Gal1-H4	2.4 ± 0.2	2.2 ± 0.2	2.29 ± 0.20	2.29 ± 0.20	2.29 ± 0.21	2.11 ± 0.13
Gal1-HO2	Glc-H61		3.6 ± 0.4	3.54 ± 1.07	3.50 ± 1.08	3.46± 1.07	4.27 ± 1.47
Gal1-HO2	Glc-H62		3.4 ± 0.3	3.70 ± 1.00	3.63 ± 1.01	3.63 ± 1.00	4.97 ± 0.72
Gal1-H1	Glc-HO3		3.5 ± 0.4	3.25 ± 0.64	3.25 ± 0.64	3.23 ± 0.65	3.41 ± 0.64
Gal1-H1	Glc-HO6		>4	3.52 ± 1.06	3.50 ± 1.06	3.49 ± 1.07	3.90 ± 0.59

Table S5: Intra- and inter-residue hydrogen bond occupancies and their standard errors for all systems obtained from MD simulations.

Donor-Acceptor Pairs	$GM1^{10\%}$	$GM1^{20\%}$	$GM1^{30\%}$
CER--POPC			
OH--O	2.4 ± 0.3	2 ± 0.4	1.6 ± 0.2
NH--O	41 ± 1.6	42.4 ± 1.1	39.9 ± 1.4
CER--CER			
OH--O	1.2 ± 0.4	1.1 ± 0.4	1.6 ± 0.2
NH--O	10.8 ± 2.6	15.8 ± 3.1	26 ± 2.5
CARB--POPC			
Glc-POPC	20.9 ± 0.5	19.3 ± 0.3	18 ± 0.3
Gal1-POPC	5.8 ± 0.3	6.5 ± 0.2	7.1 ± 0.4
GalNAc-POPC	0.8 ± 0.1	0.9 ± 0.1	1.3 ± 0.2
Gal2-POPC	1.3 ± 0.1	1.3 ± 0.2	2.1 ± 0.3
Neu5Ac-POPC	3.6 ± 0.1	3.9 ± 0.2	4.5 ± 0.2
CARB--CER			
Glc-CER	14.8 ± 0.3	14.9 ± 0.6	15.6 ± 0.6
Gal1-CER	0 ± 0.0	0.1 ± 0.0	1.2 ± 0.2
GalNAc-CER	0 ± 0.0	0.3 ± 0.1	0 ± 0.0
Gal2-CER	0.8 ± 0.3	0.1 ± 0.0	1 ± 0.3
Neu5Ac-CER	0.3 ± 0.1	0.6 ± 0.2	0.5 ± 0.1
CARB--CARB (Inter segment)			
Glc-CARB	0.8 ± 0.1	2.3 ± 0.2	3.6 ± 0.2
Gal1-CARB	1.7 ± 0.5	3.5 ± 0.2	5.9 ± 0.2
GalNAc-CARB	1.5 ± 0.1	3.6 ± 0.2	6.1 ± 0.3
Gal2-CARB	1.9 ± 0.1	3.9 ± 0.1	6.5 ± 0.1
Neu5Ac-CARB	2.8 ± 0.4	6.6 ± 0.1	10.4 ± 0.3
CARB--CARB (Intra segment)			
Glc-CARB	9.1 ± 0.2	10.2 ± 0.3	11.7 ± 0.2
Gal1-CARB	27.7 ± 0.3	28.6 ± 0.3	30.2 ± 0.4
GalNAc-CARB	10.8 ± 0.3	13.6 ± 0.3	16.3 ± 0.4
Gal2-CARB	4.2 ± 0.1	6.4 ± 0.1	9 ± 0.1
Neu5Ac-CARB	25.9 ± 0.3	29.9 ± 0.2	33.8 ± 0.4

Table S6: Average bilayer thickness d_H (Å) of ordered and disordered bilayer regions for larger systems.[a] The bilayer regions are categorized into three classes based on the local bilayer properties from a pair of the nearest neighboring lipids in top and bottom leaflets (see Methods): ordered (both lipids from ordered lipid clusters), intermediate (only one lipid from ordered lipid cluster), and disordered (none of them from the ordered lipid clusters).

System	Ordered	Intermediate	Disordered
$GM1^{10\%B}$	32.1 ± 0.1	30.2 ± 0.1	28.3 ± 0.0
$GM1^{20\%B}$	34.9 ± 0.1	31.2 ± 0.1	27.6 ± 0.1
$GM1^{30\%B}$	36.5 ± 0.1	30.9 ± 0.1	25.5 ± 0.1
$GM1^{10\%B\text{-}330K}$	29.2 ± 0.2	28.5 ± 0.1	27.7 ± 0.0
$GM1^{20\%B\text{-}330K}$	30.0 ± 0.1	29.0 ± 0.0	28.2 ± 0.0
$GM1^{30\%B\text{-}330K}$	30.2 ± 0.1	29.2 ± 0.0	28.3 ± 0.0

[a]Average d_H and its standard error (numbers in parenthesis) are calculated over six 50-ns blocks for $GM1^{10\%B}$, four 50-ns blocks for $GM1^{20\%B}$, two 50-ns blocks for $GM1^{30\%B}$, and three 50-ns blocks for $GM1^{10\%B\text{-}330K}$, $GM1^{20\%\text{-}330K}$, and $GM1^{30\%\text{-}330K}$.

FIGURES

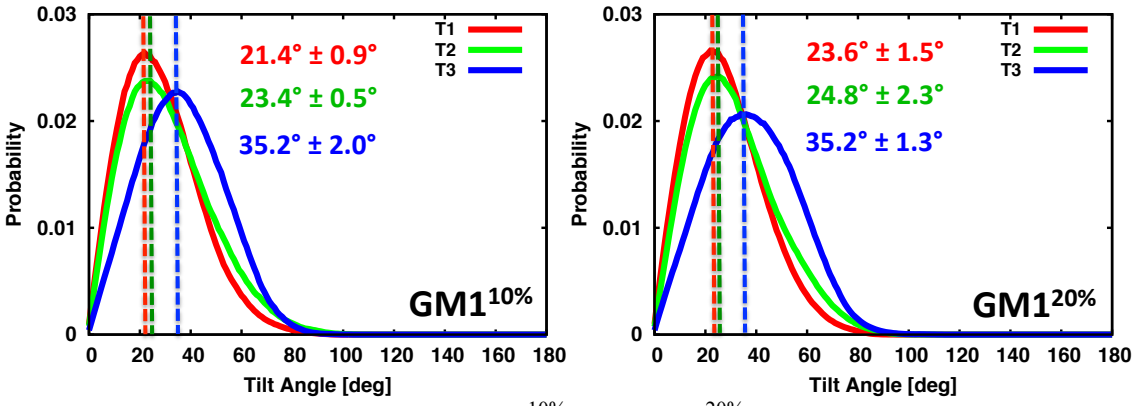

Figure S1: Tilt angle distributions in $GM1^{10\%}$ and $GM1^{20\%}$ with the peak tilt angles. T1 is a vector from the C1 carbon of residue Glc and the C4 carbon of GalNAc, T2 a vector from the C1 carbon of residue Glc and the C4 carbon of residue Gal2, and T3 a vector from C1 carbon of residue Glc and the C5 carbon of residue Neu5Ac.

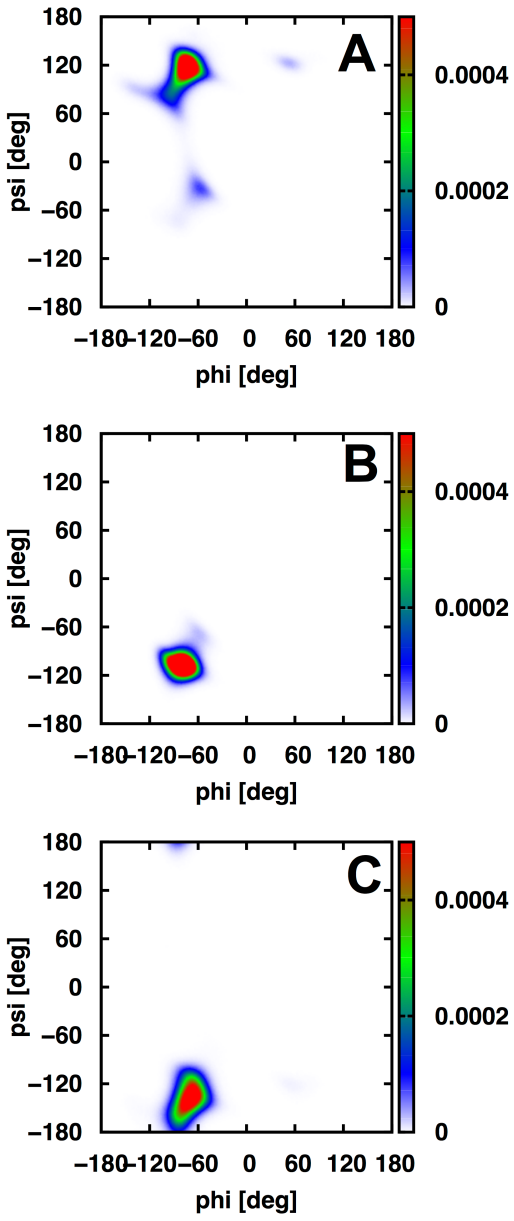

Figure S2: (A) β–Gal–(1→4)–β–Glc (ϕ_1/ψ_1), (B) β–GalNAc–(1→4)–β–Gal (ϕ_2/ψ_2), and (C) β–Gal–(1→3)–β–GalNAc (ϕ_3/ψ_3) torsion distribution of GM1 oligosaccharide in GM1$^{30\%}$.

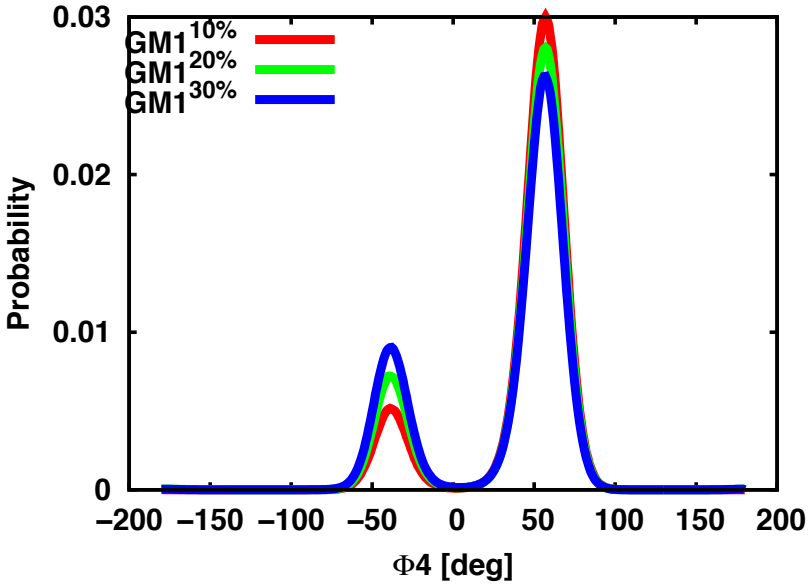

Figure S3: ϕ_4 torsion angles distribution of GM1 oligosaccharide in $GM1^{10\%}$, $GM1^{10\%}$, and $GM1^{30\%}$.

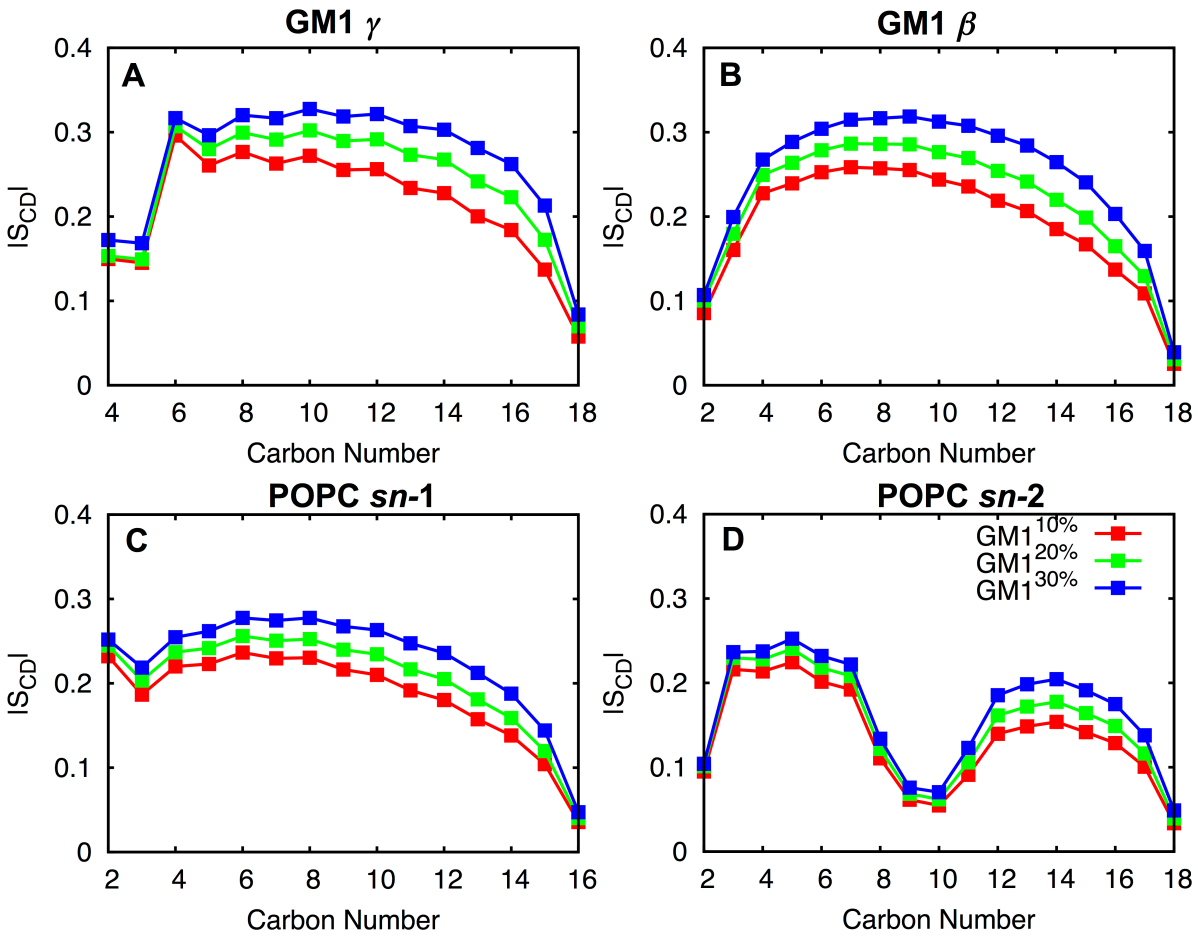

Figure S4: (A and B) The calculated GM1 γ and β chain order parameters and (C and D) POPC *sn*-1 and *sn*-2 chain order parameters in $GM1^{10\%}$, $GM1^{20\%}$, and $GM1^{30\%}$. The color ticks for all systems are given in (D).

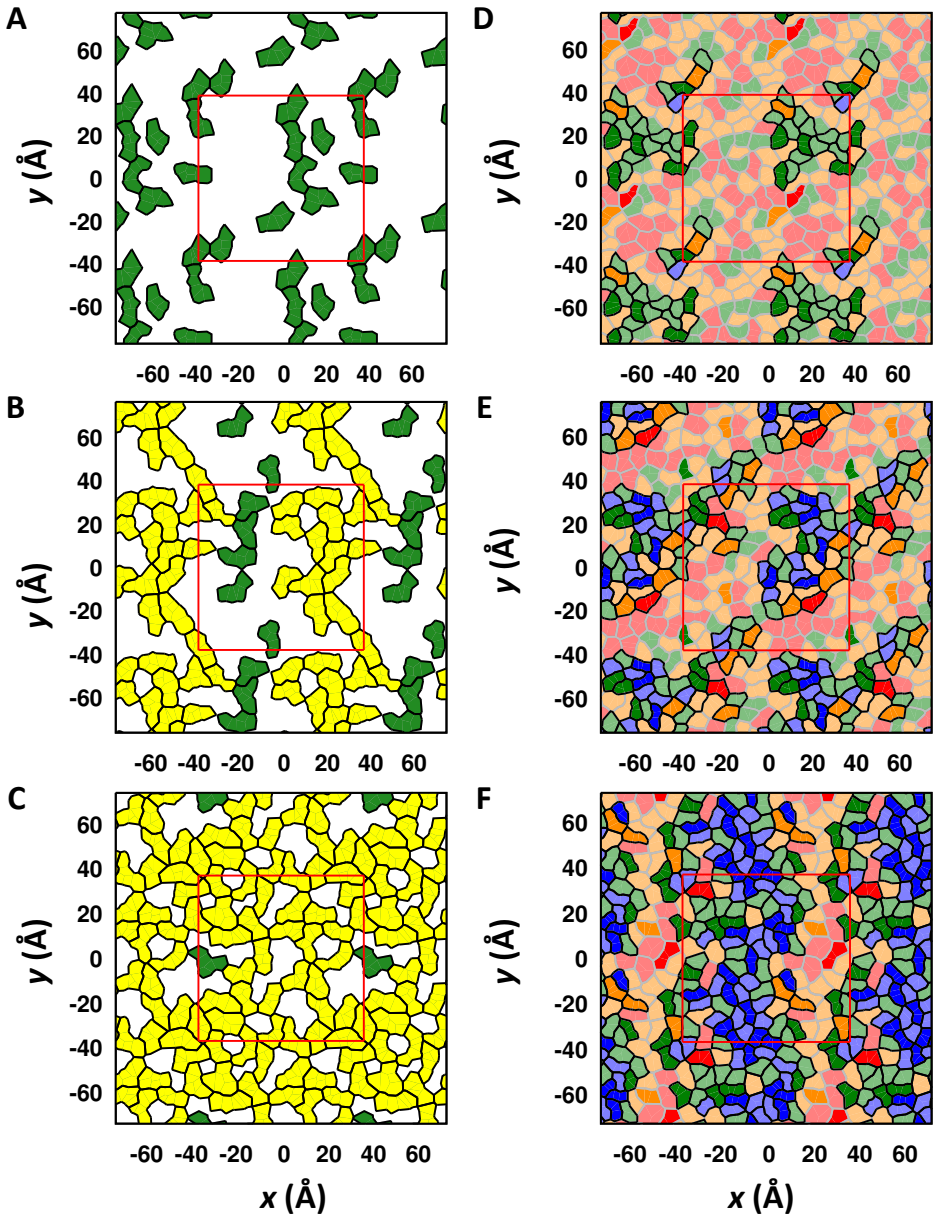

Figure S5: (A-C) Snapshots of carbohydrate clusters in (A) $GM1^{10\%}$, (B) $GM1^{20\%}$, and (C) $GM1^{30\%}$. Finite-sized carbohydrate clusters are shown in green and percolated one is shown in yellow, where five monosaccharides from the same GM1 are enclosed by black border. (D-F) Snapshots of ordered lipid clusters illustrating the spatial distribution of ordered lipids in (D) $GM1^{10\%}$, (E) $GM1^{20\%}$, and (F) $GM1^{30\%}$. The ordered states are mapped onto Voronoi tessellation of lipid tails with different colors: the highest (blue), upper-intermediate (green), lower-intermediate (orange), and the lowest ordered state (red). The POPC Voronoi regions are mapped with lighter color to distinguish from GM1 regions. The lipids in ordered-lipid clusters are enclosed by black border. The primary cell (simulation box) is indicated by a red box.

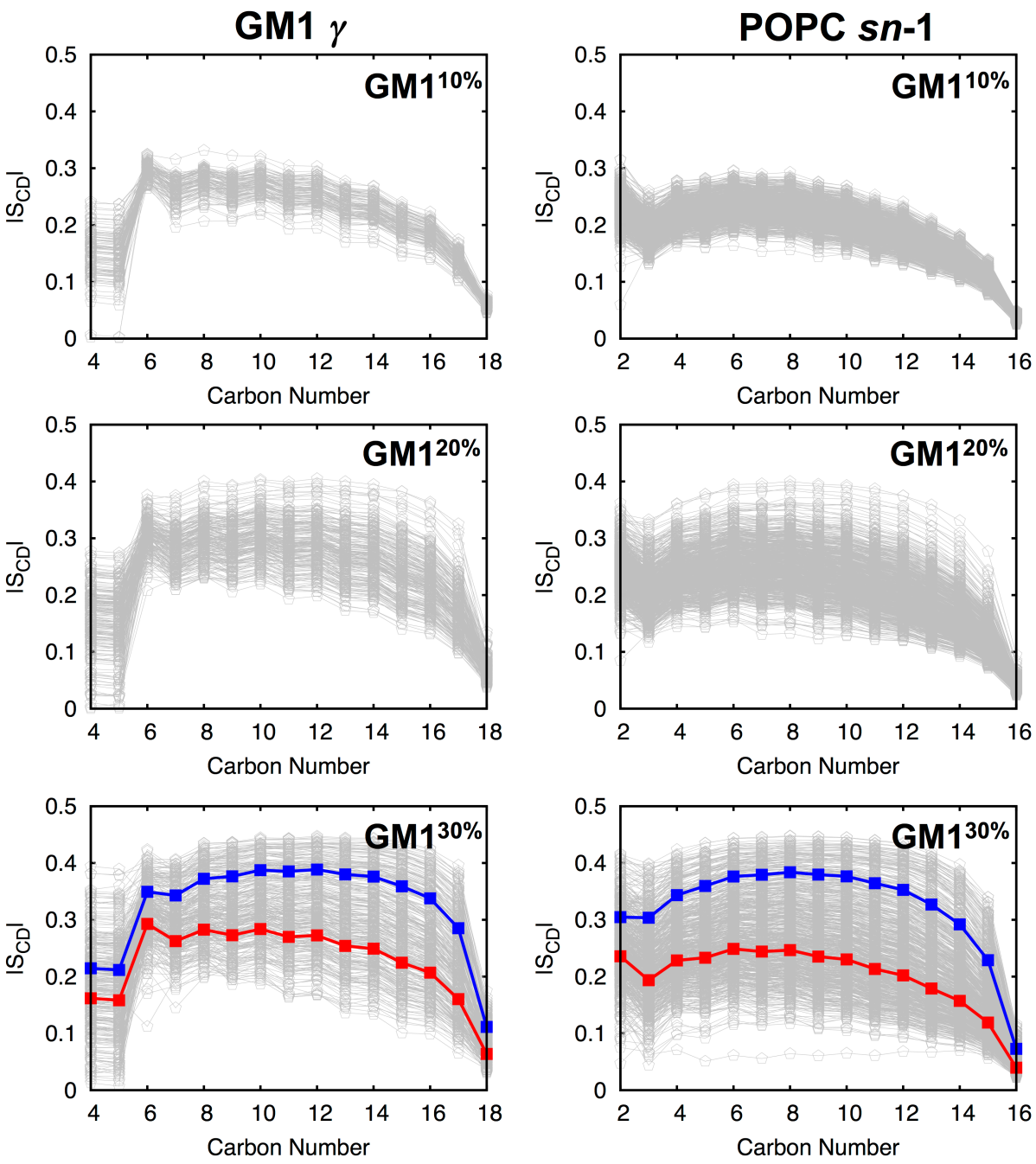

Figure S6: The overlay of the GM1 γ and POPC *sn*-1 chain order parameters in $GM1^{10\%}$, $GM1^{20\%}$, and $GM1^{30\%}$ along with average chain order parameters for high ordered (blue) and low ordered (red) chains in $GM1^{30\%}$. The overlay of the GM1 β and POPC *sn*-2 chain order parameters shows same trend.

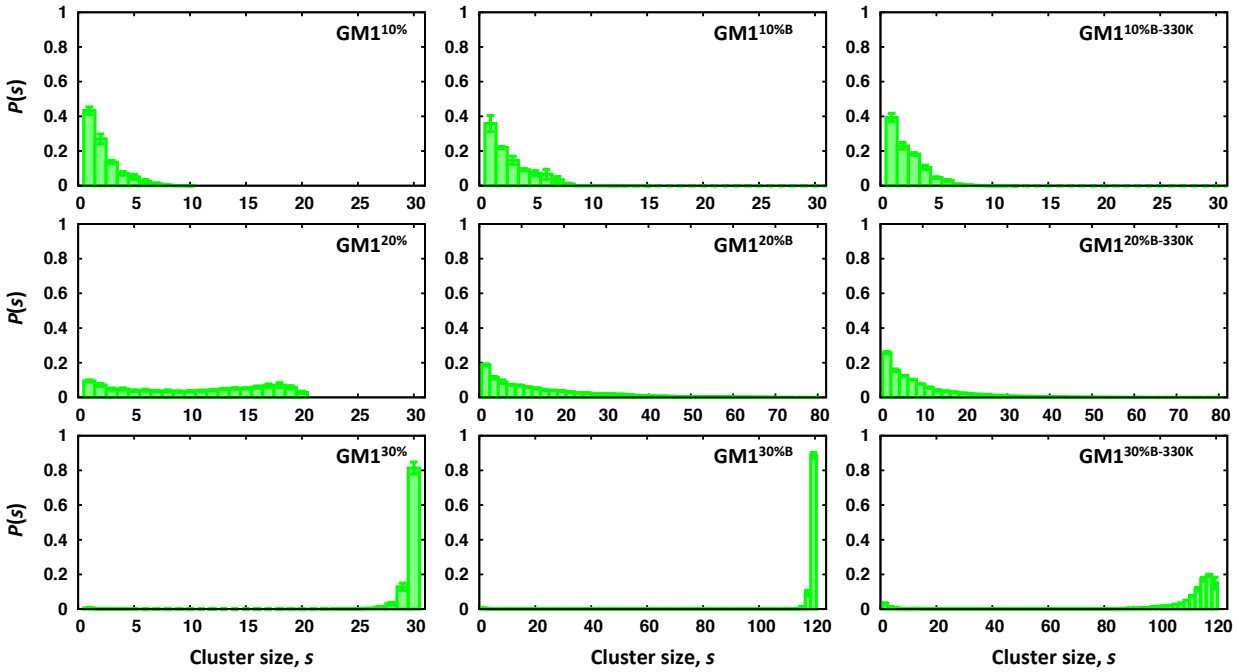

Figure S7: Probability that a GM1 belongs to a cluster of size s, $P(s)$. The bin size is one for small systems (left panels) and those at 10% GM1 concentrations (top panels). For the other systems, the bin size is two.

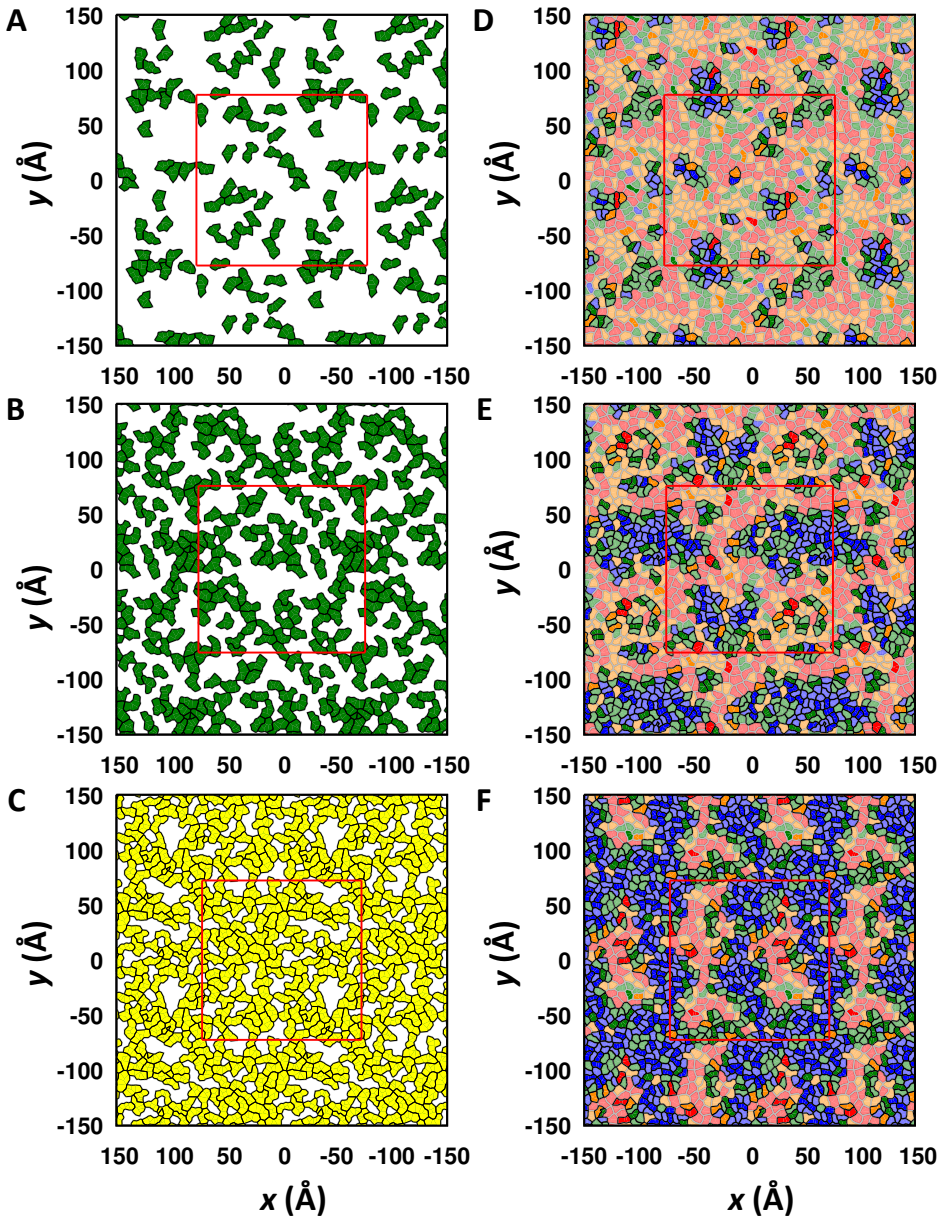

Figure S8: (A-C) Snapshots of carbohydrate clusters in (A) $GM1^{10\%B}$, (B) $GM1^{20\%B}$, and (C) $GM1^{30\%B}$. Finite-sized carbohydrate clusters are shown in green and percolated one is shown in yellow, where five monosaccharides from the same GM1 are enclosed by black border. (D-F) Snapshots of ordered lipid clusters illustrating the spatial distribution of ordered lipids in (D) $GM1^{10\%B}$, (E) $GM1^{20\%B}$, and (F) $GM1^{30\%B}$. The ordered states are mapped onto Voronoi tessellation of lipid tails with different colors: the highest (blue), upper-intermediate (green), lower-intermediate (orange), and the lowest ordered state (red). The POPC Voronoi regions are mapped with lighter color to distinguish from GM1 regions. The lipids in ordered-lipid clusters are enclosed by black border. The primary cell (simulation box) is indicated by a red box.

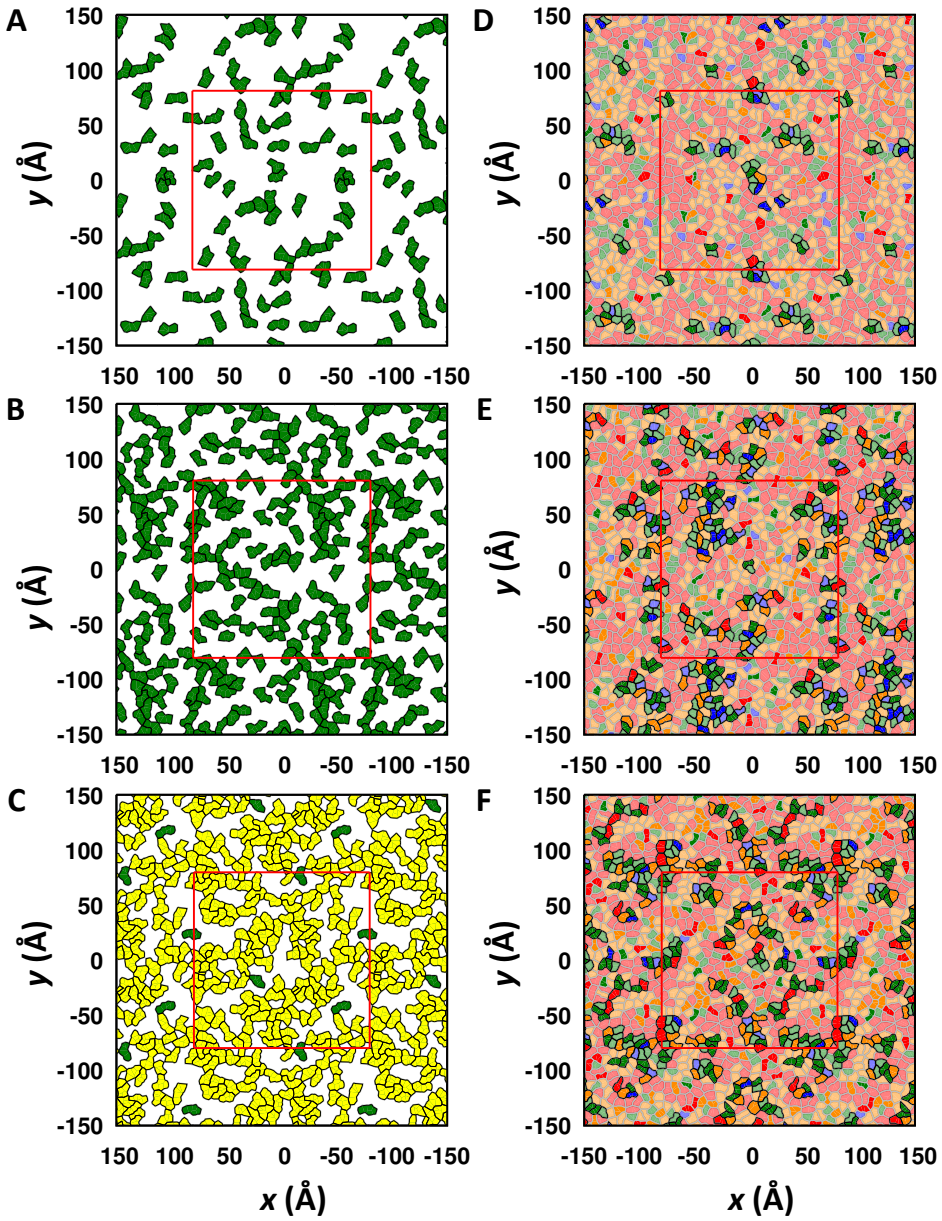

Figure S9: (A-C) Snapshots of carbohydrate clusters in (A) $GM1^{10\%B\text{-}330K}$, (B) $GM1^{20\%B\text{-}330K}$, and (C) $GM1^{30\%B\text{-}330K}$. Finite-sized carbohydrate clusters are shown in green and percolated one is shown in yellow, where five monosaccharides from the same GM1 are enclosed by black border. (D-F) Snapshots of ordered lipid clusters illustrating the spatial distribution of ordered lipids in (D) $GM1^{10\%B\text{-}330K}$, (E) $GM1^{20\%\text{-}330K}$, and (F) $GM1^{30\%B\text{-}330K}$. The ordered states are mapped onto Voronoi tessellation of lipid tails with different colors: the highest (blue), upper-intermediate (green), lower-intermediate (orange), and the lowest ordered state (red). The POPC Voronoi regions are mapped with lighter color to distinguish from GM1 regions. The lipids in ordered-lipid clusters are enclosed by black border. The primary cell (simulation box) is indicated by a red box.